An ambiphilic phosphine/H-bond donor ligand and its application to the gold mediated cyclization of propargylamides

Srobona Sen and François P. Gabbaï*

Department of Chemistry, Texas A&M University, College Station, TX 77843-3255.

SUPPORTING INFORMATION

This PDF file includes:

Synthesis of **1**

Synthesis of **2**

Synthesis of **3**

Figure S1. ^{1}H NMR spectrum of **1** in $CDCl_3$

Figure S2. ^{13}C NMR spectrum of **1** in $CDCl_3$

Figure S3. ^{19}F NMR spectrum of **1** in $CDCl_3$

Figure S4. . ^{31}P NMR spectrum of **1** in $CDCl_3$

Figure S5. ^{1}H NMR spectrum of **2** in $CDCl_3$

Figure S6. ^{13}C NMR spectrum of **2** in $CDCl_3$

Figure S7. ^{19}F NMR spectrum of **2** in $CDCl_3$

Figure S8. ^{31}P NMR spectrum of **2** in $CDCl_3$

Figure S9. ^{1}H NMR of an equimolar solution of **2** and **A** and ^{31}P NMR spectrum of **2** in CD_3CN

Figure S10. ^{1}H NMR spectrum of **3** in $CDCl_3$

Figure S11. ^{13}C NMR spectrum of **3** in $CDCl_3$

Figure S 12. ^{19}F NMR spectrum of **3** in $CDCl_3$

Figure S 13. ^{31}P NMR spectrum of **3** in $CDCl_3$

Figure S14. Variable Temperature ^{31}P NMR spectra of 2 in CD_2Cl_2.

Figure S15. Decay of NMR signal intensity with the progressive increase of the gradient strength and the plot of $\ln(I/I_0)$ vs G^2 for the reference compound **A** (1,3,5-tri-*tert*-butylbenzene) and **2** as obtained from the PGSE experiment.

Figure S16. The plot of $\ln(I/I_0)$ vs G^2 for the reference compound **A** (1,3,5-tri-*tert*-butylbenzene) and **2** as obtained from the PGSE experiment after three-fold and nine-fold dilution.

Figure S17. ESI-MS^- spectra of **1** and **2**.

Figure S18. GC trace obtained for the cyclization of *N*-(prop-2-yn-1-yl)-benzamide catalyzed by **2** in CH_2Cl_2.

Figure S19. GC trace obtained for the cyclization of N-(prop-2-yn-1-yl)-2-methylbenzamide catalyzed by **2** in CH_2Cl_2.

Figure S20. GC trace obtained for the cyclization of N-(prop-2-yn-1-yl)-4-fluorobenzamide catalyzed by **2** in CH_2Cl_2.

Figure S21. GC trace obtained for the cyclization of N-(prop-2-yn-1-yl)4-methoxybenzamide catalyzed by **2** in CH_2Cl_2.

Figure S22. ^1H NMR spectrum of N-(prop-2-yn-1-yl)-4-fluorobenzamide after the completion of the catalysis.

Figure S23. ^1H NMR spectrum of N-(prop-2-yn-1-yl)-4-fluorobenzamide after the completion of the catalysis.

Figure S24. ^1H NMR spectra obtained after 24h for the cyclization of propargylamide**s** catalyzed by **2** in CH_2Cl_2.

Table S1. Observed and calculated volumes and radii for **2**

Table S2. Conductivity of solutions of complex **2** and the reference electrolyte $TBAPF_6$

❖ **Materials and Methods:**

(tht)AuCl[1], *o*-Bromotrifluoroacetanilide[2], trifluoroacetanilide[3] and the various propargylic amides[4] were prepared according to previously reported procedures. Chloro(triphenylphosphine)gold was obtained from the reaction of (tht)AuCl with triphenylphopshine. *o*-bromoaniline, *n*BuLi (2.2M in hexane) and *t*BuLi (1.5M in pentane) were purchased from Oakwood Chemicals and Alfa Aesar and used as received. All preparations were carried out under an atmosphere of dry N_2 employing either a glove box or standard Schlenk techniques. Solvents were dried by passing through an alumina column (CH_2Cl_2, pentane) or refluxing under N_2 over Na/K (THF, Et_2O). Ambient-temperature NMR spectra were recorded using a Varian Unity Inova 500 FT NMR (499.42 MHz for ^1H, 125.58 MHz for ^{13}C, 469.93 MHz for ^{19}F, 202.17 MHz for ^{31}P) spectrometer. Chemical shifts (δ) are given in ppm and are referenced against residual solvent signals (^1H, ^{13}C) or external $BF_3 \cdot Et_2O$ (^{19}F), H_3PO_4 (^{31}P). GC analysis was carried out using an Agilent GC System (6890 Series) Plus set up equipped with a Rxi-5ms fused silica column from RESTEK (length: 15 m length, id: 0.53 mm, film thickness: 0.50 µm). The column temperature was maintained at 50 °C for 2 min and raised to 250 °C at 25 °C/min. The final temperature (250 °C) was held for 10 min. The conductivity measurements were performed using a Mettler Toledo FiveGo conductivity probe. Elemental analyses were performed by Atlantic Microlab (Norcross, GA).

❖ **Crystallography:**

The crystallographic measurements were performed at 110(2) K using a Bruker APEX-II CCD area detector diffractometer, with graphite-monochromated Mo Kα radiation (λ = 0.71069 Å) and ω scans with a 0.5° step in ω. A specimen of suitable size and quality was selected and mounted onto a nylon loop. The semiempirical method SADABS was applied for absorption correction. The structure was solved by direct methods, which successfully located most of the non-hydrogen atoms. The N-*H* atoms in **1** were located in the electron density map and refined anisotropically. All other hydrogen atoms were placed at calculated positions and refined using a riding model. Subsequent refinement on F^2 using the SHELXTL/PC package28 (version 6.1) allowed location of the remaining non-hydrogen atoms. Data reduction and further calculations were performed using the Bruker Apex2 (2013) and SHELXTL program packages.

❖ **SYNTHESIS:**

Synthesis of 1:

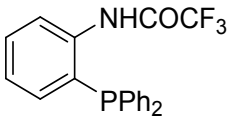

n-Butyllithium (2.2 M) in hexane (1.69 ml, 3.73 mmol) was added to a solution of *o*-bromotrifluoroacetanilide (1.0 g, 3.73 mmol) in THF (20 mL) at -78ºC. After 1 h, *t*-butyllithium (1.5 M) in pentane (4.97 ml, 7.46 mmol) was added dropwise. The mixture was stirred at -78ºC for another hour, after which PPh_2Cl (0.66 ml, 3.73 mmol) was added. The mixture was allowed to warm to room temperature and stirred overnight. The reaction mixture was quenched with an HCl solution (1M) in diethyl ether (10 ml). All volatiles were evaporated under vacuum and the resulting solid was extracted with pentane. The solvent was evaporated to afford the ligand as pale yellow solid. Yield: 974 mg, 70%. X-ray diffraction quality crystals were obtained by slow evaporation of a concentrated pentane solution. ^{1}H NMR ($CDCl_3$, 499.42 MHz): 8.85 (bs, N-*H*), 8.12 (dd, *J* = 8.2, 4.4 Hz, 1H), 7.45 (td, 1H), 7.39 (td, 6H), 7.31 (td, 4H), 7.19 (t, 1H), 7.03 (t, 1H). ^{13}C NMR ($CDCl_3$, 125.58 MHz): δ 154.75 (q, *J* = 37.3 Hz), 138.16 (d, *J* = 17.7 Hz), 134.11 (d, *J* = 2.4 Hz), 133.76 (s), 133.61 (s), 133.42 (d, *J* = 5.4 Hz), 132.03 (d, *J* = 10.2 Hz), 130.47 (s), 129.61 (s), 128.97 (d, *J* = 7.5 Hz), 128.20 (d, *J* = 12.1 Hz), 126.56 (d, *J* = 1.6 Hz), 122.21 (d, *J* = 1.6 Hz), 115.65 (q, *J* = 289.1 Hz). ^{19}F NMR ($CDCl_3$, 469.93 MHz): -76.11 (s). ^{31}P NMR ($CDCl_3$, 202.17 MHz): -21.42 (s). ESI$^-$/MS for $[C_{20}H_{14}F_3NOP]^-$: m/z calculated 372.08; found 372.0504. Elemental analysis (%) calculated for $C_{20}H_{15}F_3NOP$: C, 64.35; H, 4.05; N, 3.75. Found: C, 63.52; H, 4.37; N, 3.73.

Synthesis of 2:

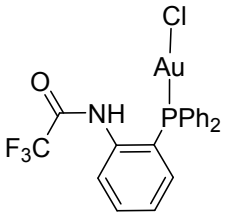

A solution of the ligand **1** (100 mg, 0.26 mmol) in THF (3 ml) was added dropwise to a suspension of (tht)AuCl (85.87 mg, 0.26 mmol) in THF (1 ml) at room temperature. It was left to stir for 2 h in a vessel protected from incident light. The reaction mixture was then layered with pentane. Over the course of 12 h, the product precipitated as a white, light-sensitive solid. The white solid was isolated by filtration and washed with pentane. The product was obtained as a light sensitive white solid. Yield: 130 mg, 83%. Vapor diffusion of pentane in a THF solution afforded clear colorless crystals of **2**. ^{1}H NMR ($CDCl_3$,

499.42 MHz): δ 8.50 (s, 1H, N-*H*), 7.85 (dd, *J* = 7.8, 4.9 Hz, 1H), 7.66 (t, *J* = 7.8 Hz, 1H), 7.63 – 7.50 (m, 10H), 7.33 (t, *J* = 7.7 Hz, 1H), 6.90 (ddd, *J* = 12.8, 7.8, 1.3 Hz, 1H). ^{13}C NMR ($CDCl_3$, 126 MHz). δ 155.02 (q, *J* = 38.2 Hz), 136.35 (d, *J* = 6.3 Hz), 134.36 (d, *J* = 14.3 Hz), 133.51 (d, *J* = 7.1 Hz), 133.28 (d, *J* = 2.0 Hz), 133.03 (d, *J* = 2.7 Hz), 129.84 (d, *J* = 12.4 Hz), 127.68 (d, *J* = 9.7 Hz), 126.95 (d, *J* = 5.4 Hz), 125.80 (s), 125.28 (s), 122.82 (s), 122.34 (s), 115.24 (q, *J* = 289.1 Hz). ^{19}F NMR ($CDCl_3$, 469.93 MHz): δ -75.69 (s). ^{31}P NMR ($CDCl_3$, 202.17 MHz): δ 22.20 (s). ESI$^-$/MS for $[C_{20}H_{14}AuClF_3NOP]^-$: m/z calculated 604.01; found 604.0068. Elemental analysis (%) calculated for $C_{20}H_{15}AuClF_3NOP$: C, 39.66; H, 2.50; N, 2.31. Found: C, 38.65; H, 2.47; N, 2.20.

Synthesis of 3

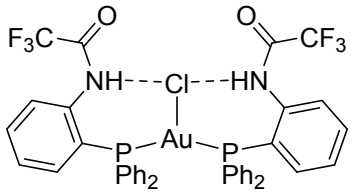

A solution of the ligand **1** (400 mg, 1.07 mmol) in THF (4 ml) was added dropwise to a suspension of (tht)AuCl (171.75 mg, 0.535 mmol) in THF (1 ml) at room temperature inside the glovebox. It was left to stir for 2 h in a vessel protected from the incident light. The solution was concentrated. Addition of pentane led to the precipitation of the product which was recovered by filtration and washed with pentane. Yield: 420 mg, 80%. Single crystals were obtained by slow diffusion of pentane into a THF solution of the complex. ^{1}H NMR (499 MHz, cdcl$_3$) δ 10.51 (s, 2H, N-*H*), 7.71 – 7.57 (m, 4H), 7.53 (dd, *J* = 11.5, 4.4 Hz, 12H), 7.41 (t, *J* = 7.6 Hz, 8H), 7.33 (t, *J* = 7.6 Hz, 2H), 6.92 (bs, 2H). ^{13}C NMR (126 MHz, cdcl$_3$) δ 156.33 (s), 156.02 (s), 137.65 (s), 134.25 (s), 133.73 (s), 132.74 (s), 132.05 (s), 129.76 (s), 129.38 (s), 128.13 (s), ^{19}F NMR ($CDCl_3$, 469.93 MHz): δ -75.15 (s). ^{31}P NMR ($CDCl_3$, 202.17 MHz): δ 35.78 (bs). Elemental analysis (%) calculated for $C_{40}H_{30}AuClF_6N_2O_2P_2$: C, 49.07; H, 3.09; N, 2.86. Found: C, 48.21; H, 3.13; N, 2.75.

❖ **Catalytic cyclization of propargylic amides in CH_2Cl_2:**

5 mol% freshly prepared **2** (5 mg, 0.00825 mmol) was added to a solution of the appropriate propargylic amide (0.1650 mmol) in 2 mL CH_2Cl_2 in a 20 mL vial. The progress of the reaction was monitored by injecting an aliquot of 10 μL in the GC spectrometer and the gas chromatogram was recorded for 18 min at 250°C.

❖ **NMR Spectra:**

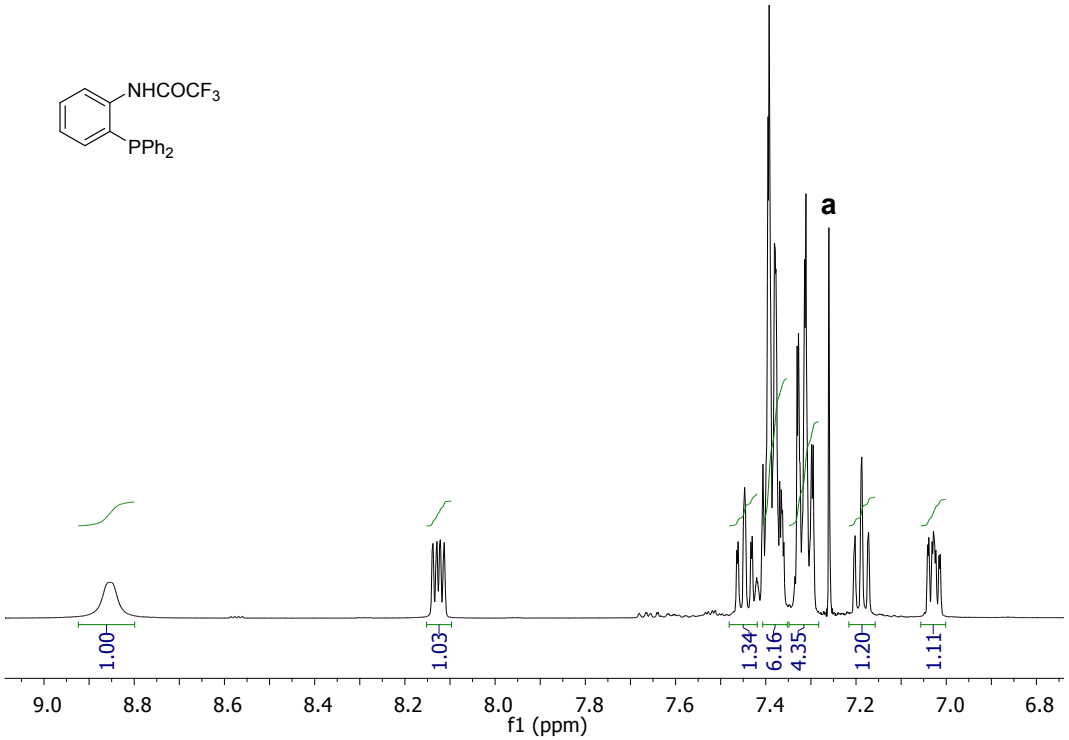

Figure S1. ^{1}H NMR spectrum of **1** in $CDCl_3$. Residual solvent peak is shown in the spectrum. **a**) $CHCl_3$

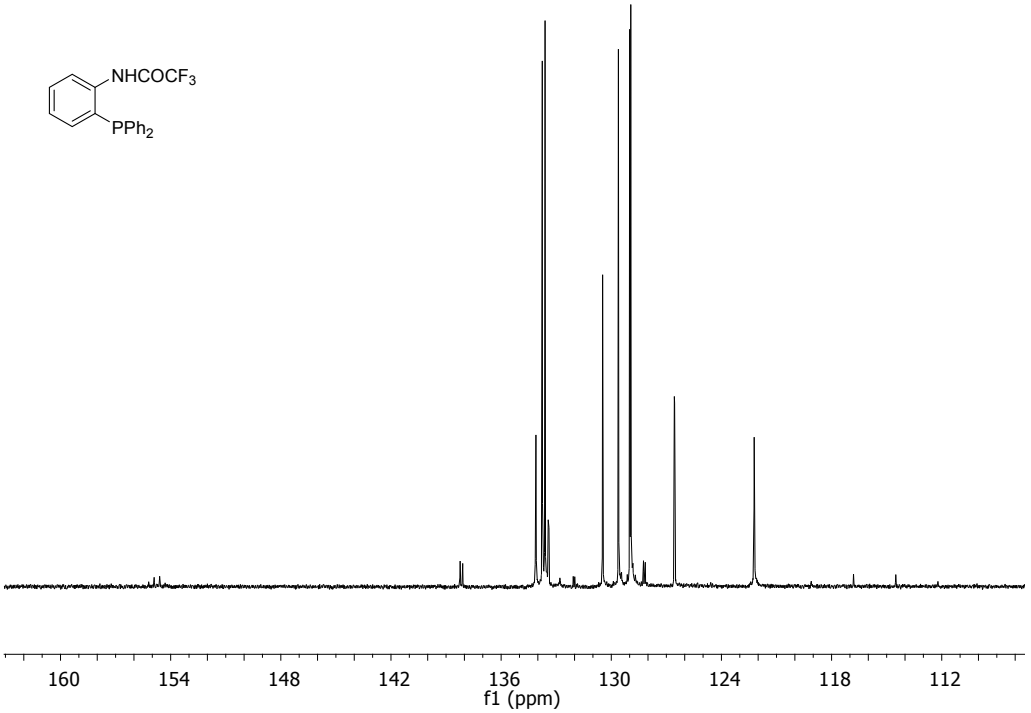

Figure S2. ^{13}C NMR spectrum of **1** in $CDCl_3$.

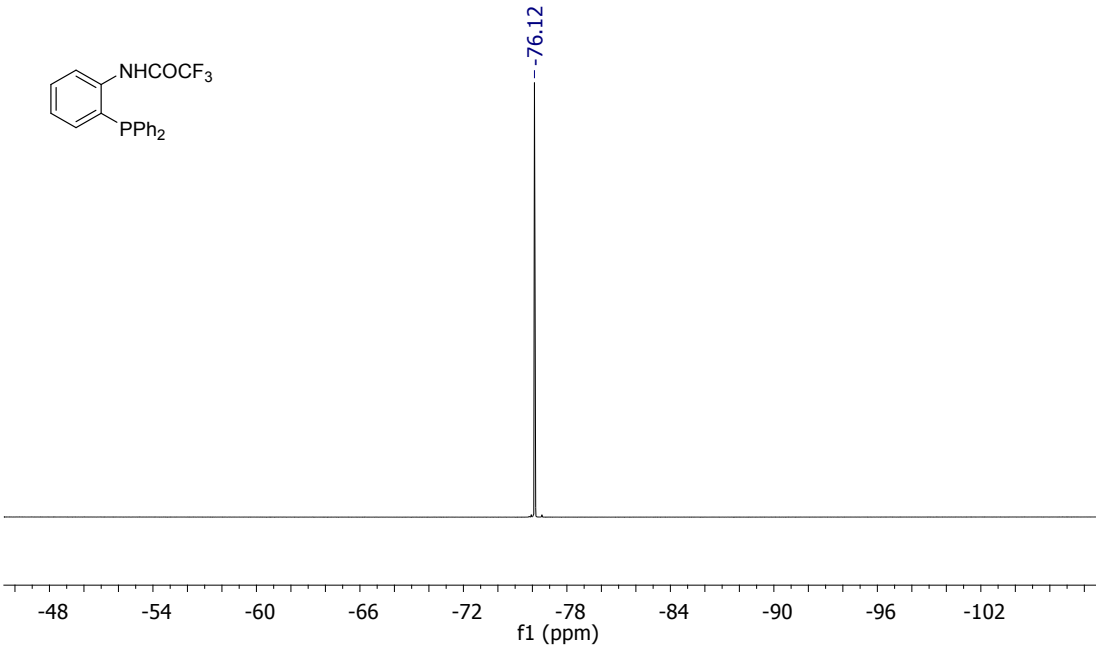

Figure S3. ^{19}F NMR spectrum of **1** in $CDCl_3$.

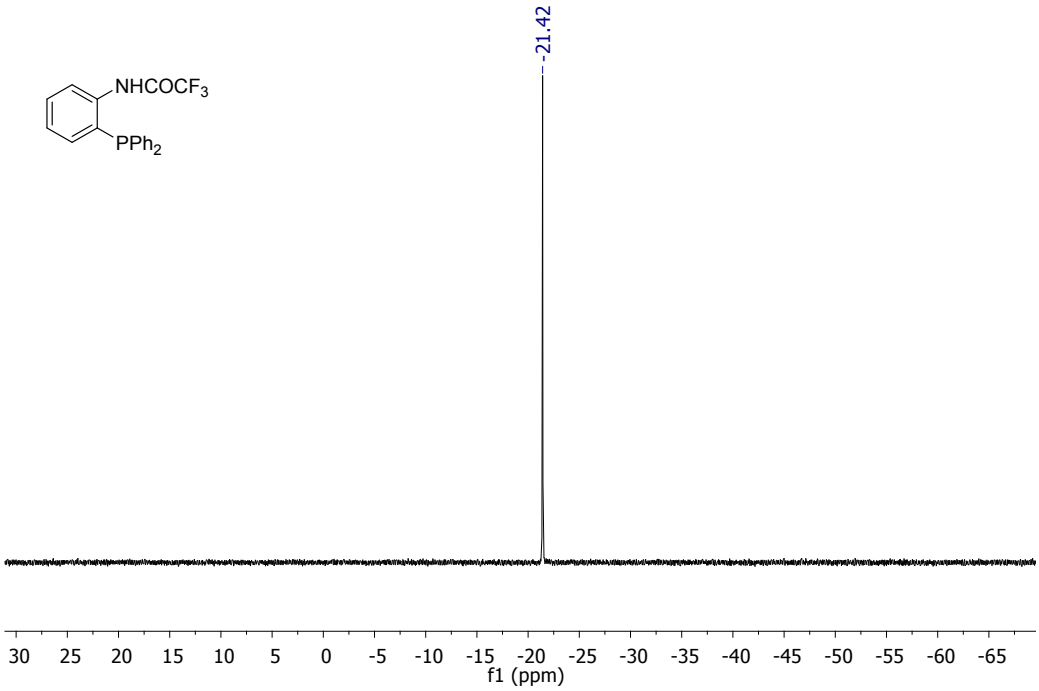

Figure S4. ^{31}P NMR spectrum of **1** in $CDCl_3$.

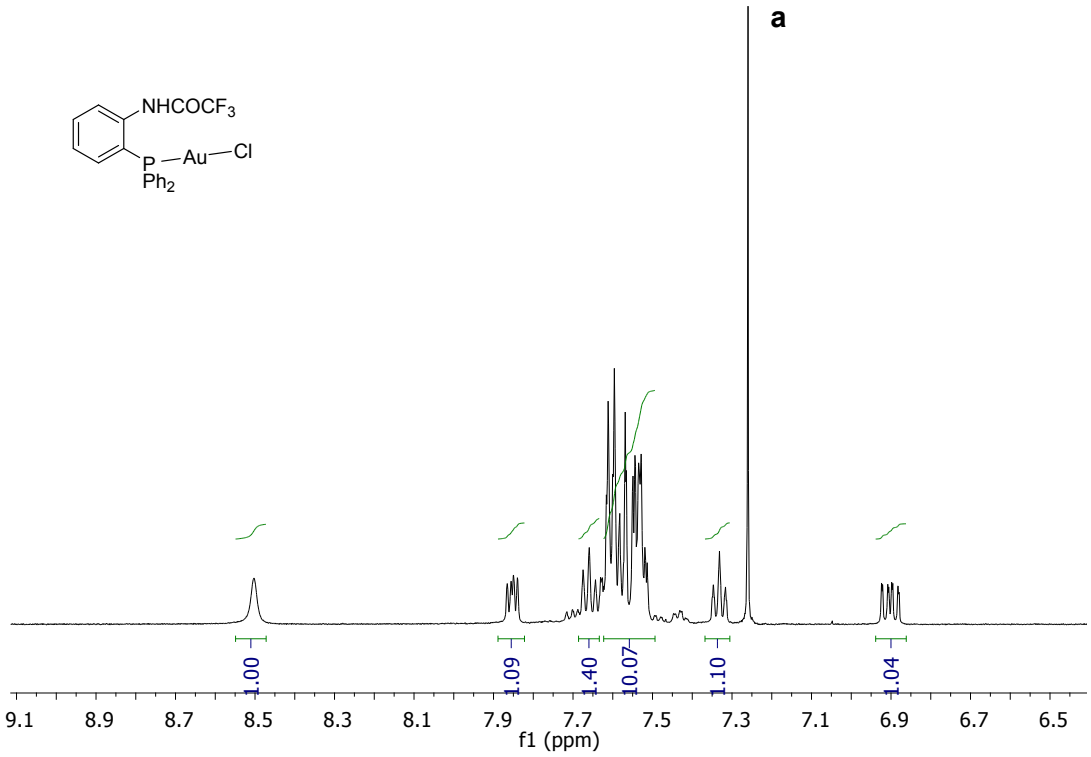

Figure S 5. ^{1}H NMR spectrum of **2** in $CDCl_3$. Residual solvent peak is shown in the spectrum. **a**) $CHCl_3$

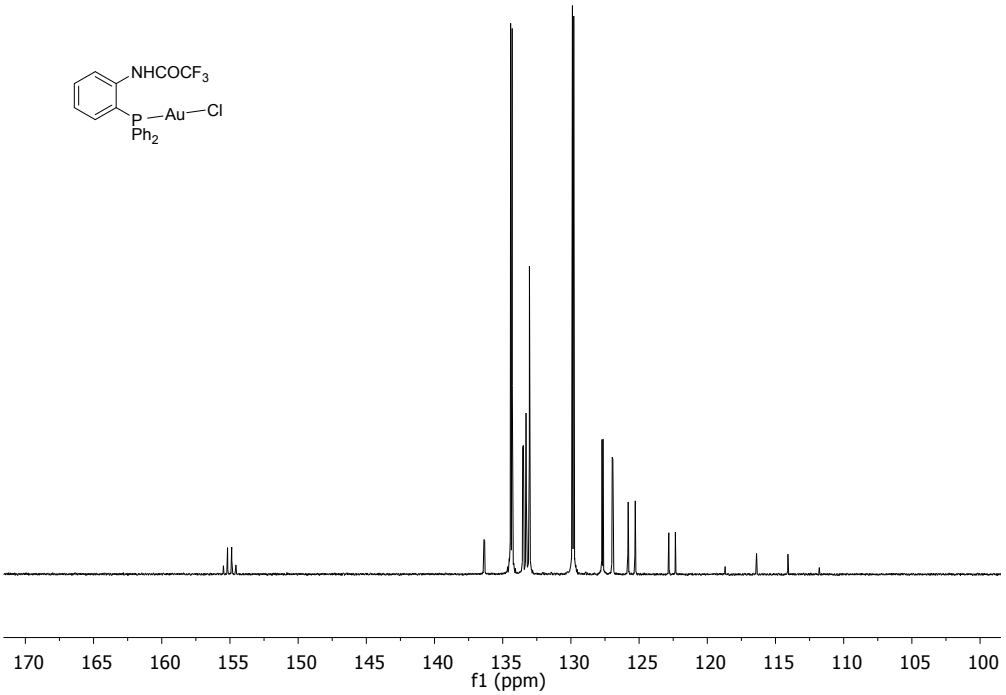

Figure S 6. ^{13}C NMR spectrum of **2** in $CDCl_3$.

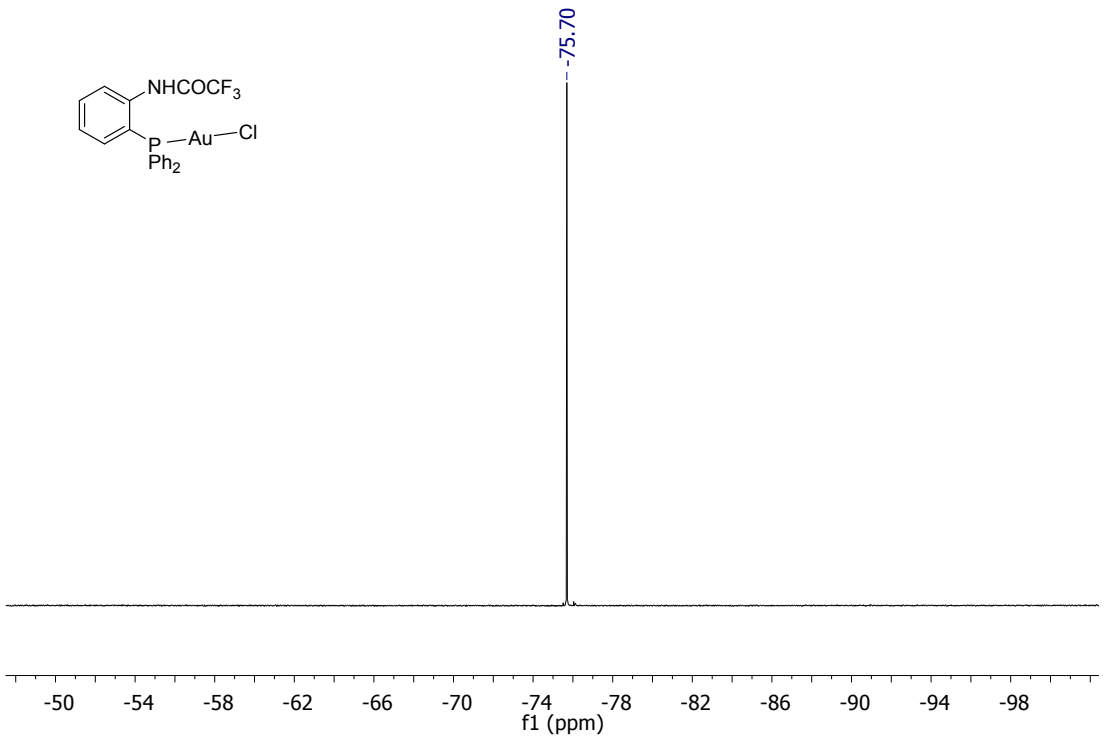

Figure S7. ^{19}F NMR spectrum of **2** in $CDCl_3$.

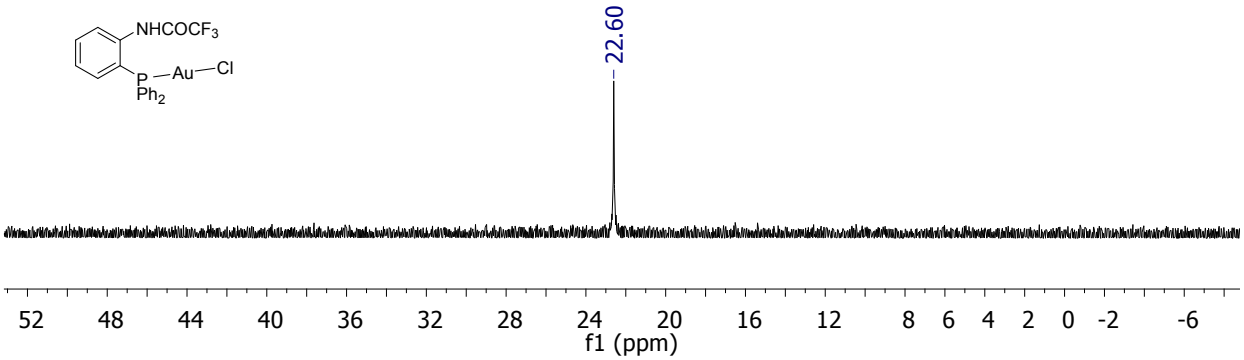

Figure S8. ^{31}P NMR spectrum of **2** in $CDCl_3$.

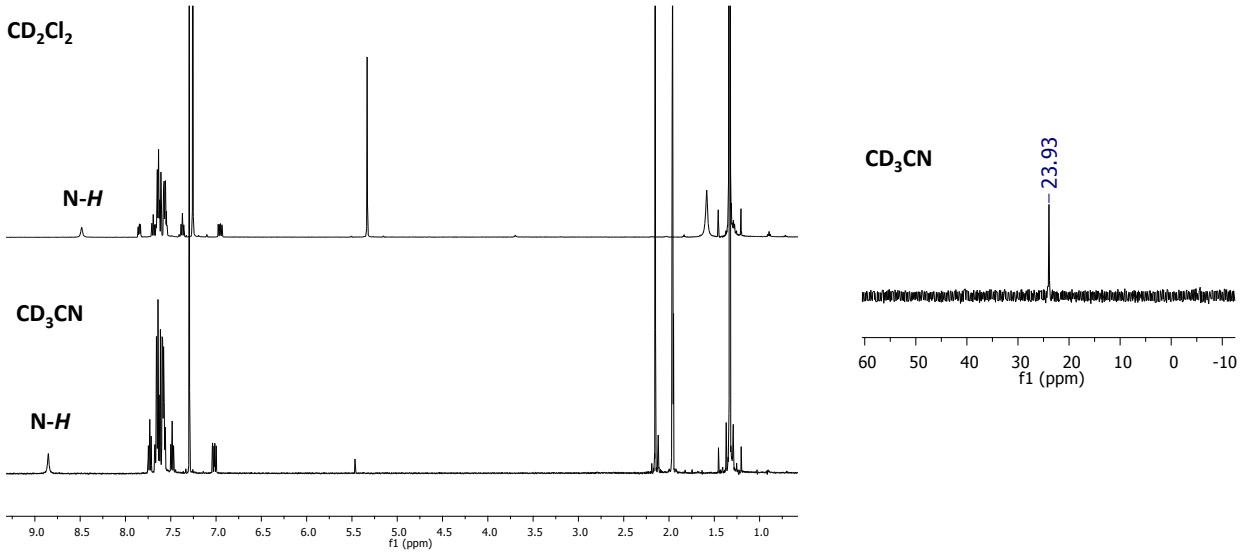

Figure S9. ^{1}H NMR spectra of an equimolar solution of **2** and **A** in CD_2Cl_2 and CD_3CN (left) and ^{31}P NMR spectrum of **2** in CD_3CN (right).

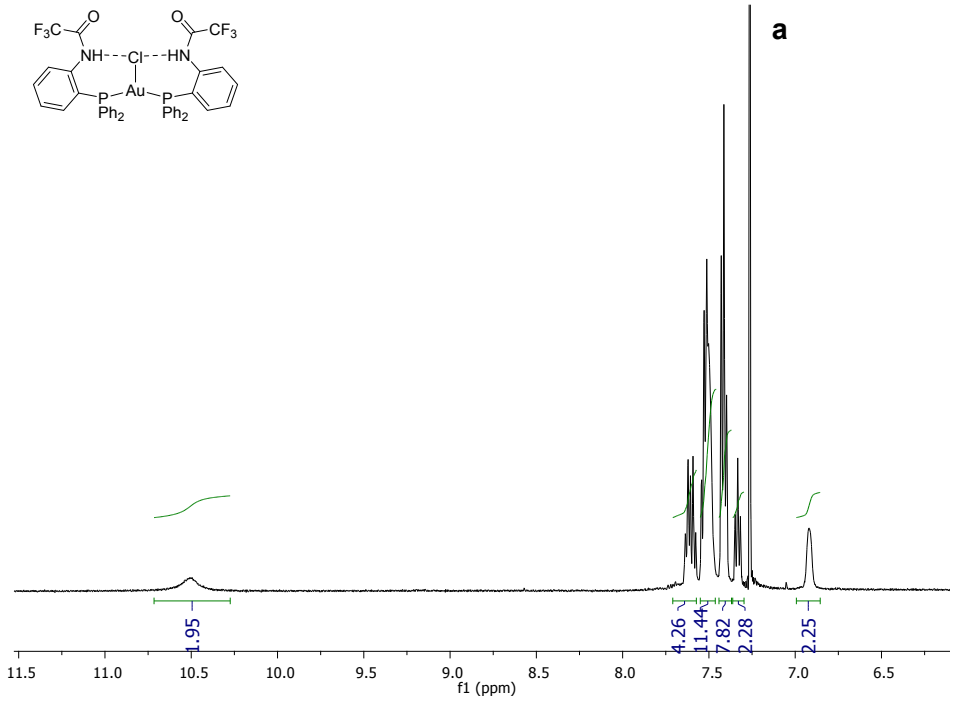

Figure S10. ^{1}H NMR spectrum of **3** in $CDCl_3$. Residual solvent peak is shown in the spectrum. **a**) $CHCl_3$

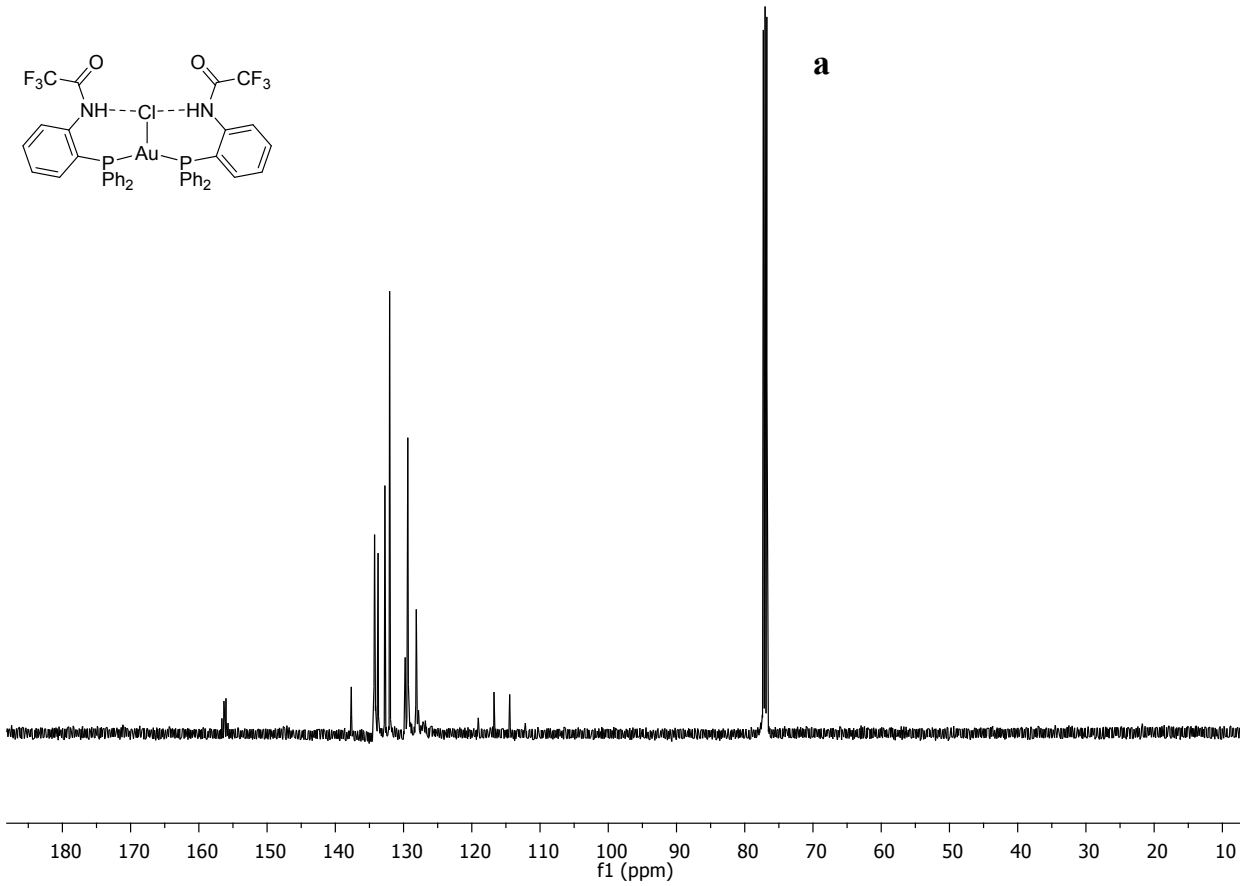

Figure S11. ^{13}C NMR spectrum of **3** in $CDCl_3$. Residual solvent peak is shown in the spectrum. **a**) $CHCl_3$

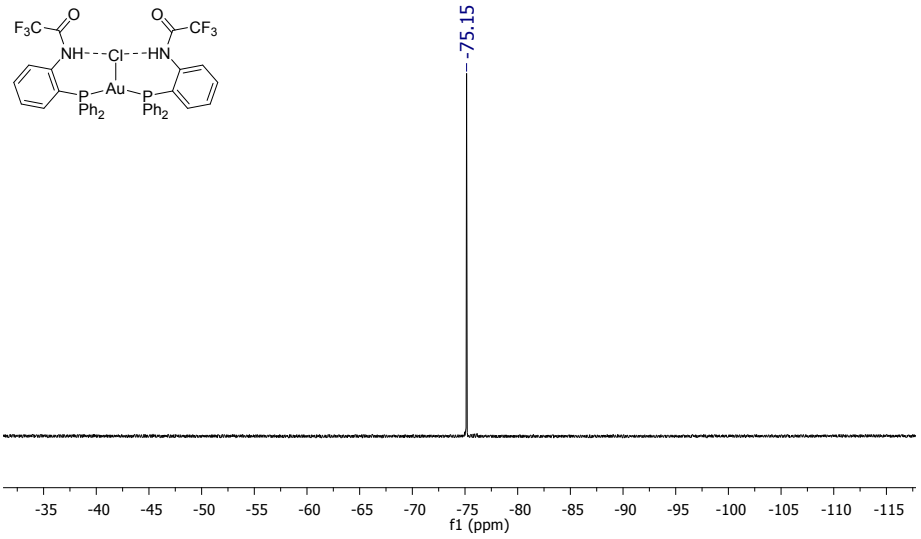

Figure S 12. ^{19}F NMR spectrum of **3** in $CDCl_3$.

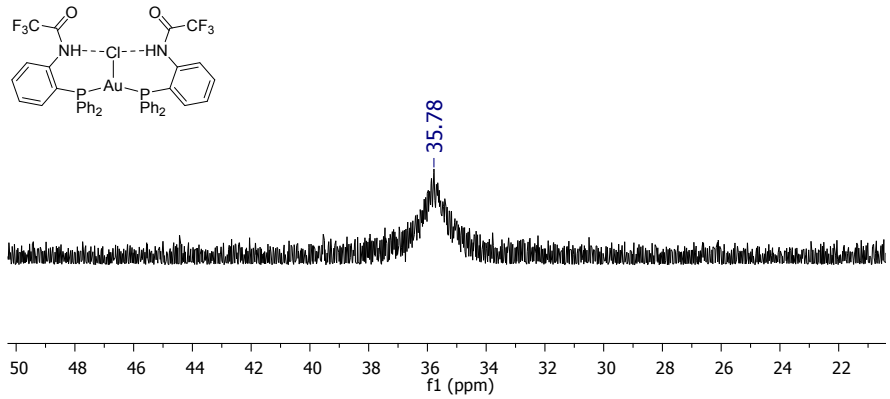

Figure S 13. ^{31}P NMR spectrum of **3** in $CDCl_3$.

❖ VARIABLE TEMPERATURE NMR

The VT ^{31}P NMR of a 0.012 M solution of **2** in CD_2Cl_2 was recorded at -30°C, -20°C, -10°C, 0°C, 10°C, 20°C, 30°C, 40°C and 50°C using a Varian Unity Inova 400 FT NMR (399.59 MHz for ^{1}H, 100.45 MHz for ^{13}C, 375.89 MHz for ^{19}F, 161.74 MHz for ^{31}P) spectrometer.

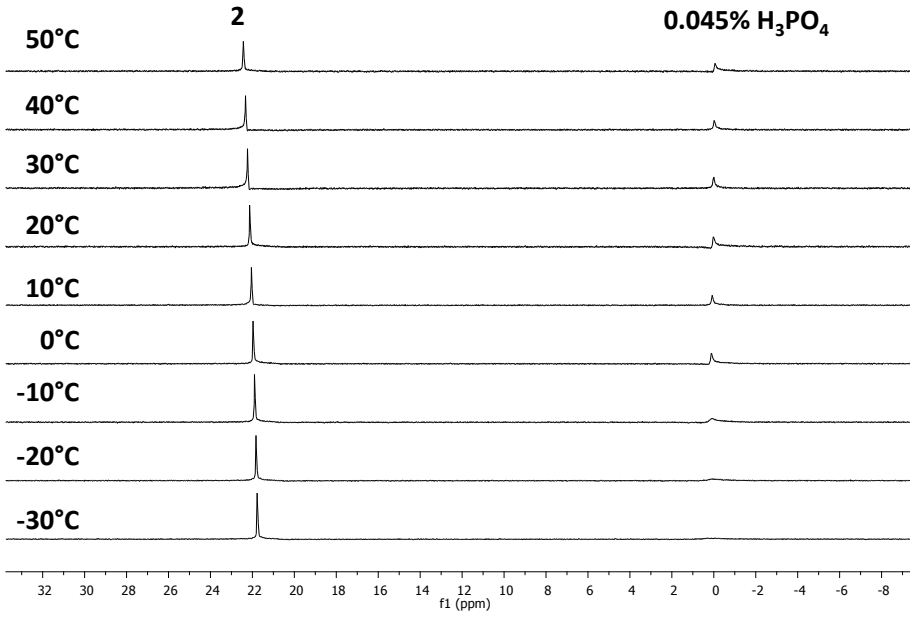

Figure S14. Variable Temperature ^{31}P NMR spectra of **2** in CD_2Cl_2.

❖ DETERMINATION OF RELATIVE RATE OF DIFFUSION OF 2 VIA PGSE EXPERIMENT IN CD_2CL_2 WITH 1,3,5-TRI-*TERT*-BUTYLBENZENE AS A REFERENCE

An NMR tube was charged with 13.2 mg (0.0218 mmol) of **2**, 5.37 mg (0.0218 mmol) of 1,3,5-tri-*tert*-butylbenzene (**A**) and 0.6 mL CD_2Cl_2. The resulting solution was subjected to Pulse Gradient Spin Echo measurements using a Varian Unity Inova 400MHz spectrometer. The gradient strength was incremented in 15 steps from 80 Dac to 2045 Dac. The relevant parameters for the experiment were: $\Delta = 30$ ms, $\delta = 1.3$ ms, d1= 2s. The measurements were repeated after a three-fold and nine-fold dilution using the same experimental parameters.

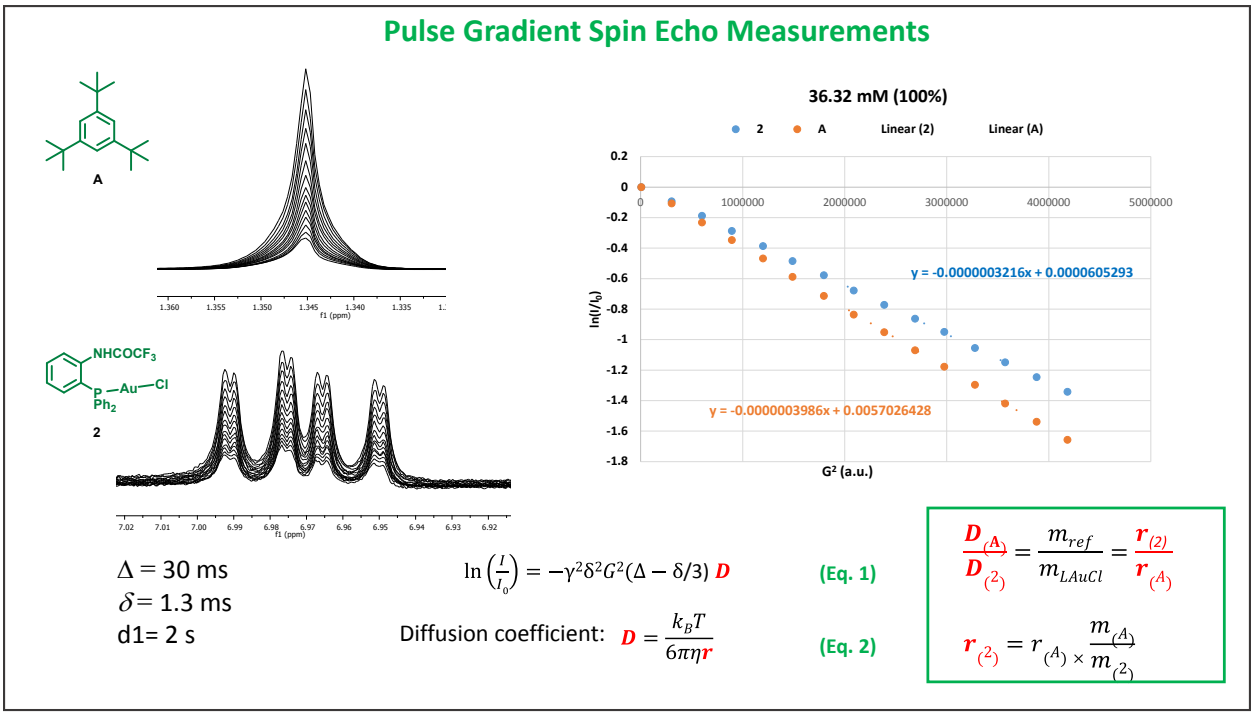

Figure S15. Left: Decay of NMR signal intensity with the progressive increase of the gradient strength. **Right:** Plot of $\ln(I/I_0)$ vs G^2 for the reference **A** (1,3,5-tri-*tert*-butylbenzene) and **2** in the same graph.

According to the Stokes-Einstein equation (Eq. 2), the ratio of the slopes is inversely proportional to the ratio of the corresponding radii. The radius of **2** was determined from the ratio of slopes and the reported value of the radius of 1,3,5-tri-*tert*-butylbenzene.

$\mathbf{V}_{\text{X-ray}}(\mathbf{2}) = 504$ Å^3

$\boldsymbol{r}_{\text{X-ray}}(\mathbf{2}) = 4.94$ Å

$\mathbf{V}_{\text{X-ray}}(\mathbf{A}) = 454$ Å^3

$r_{\text{X-ray}}(\mathbf{A}) = 4.77$ Å

r_{PGSE} (**2**, 36 mM) = 4.77 × (39.86/32.16) Å = 5.91 Å

V_{PGSE} (**2**, 36 mM) = $\frac{4}{3}\pi r^3$ = 865 Å^3

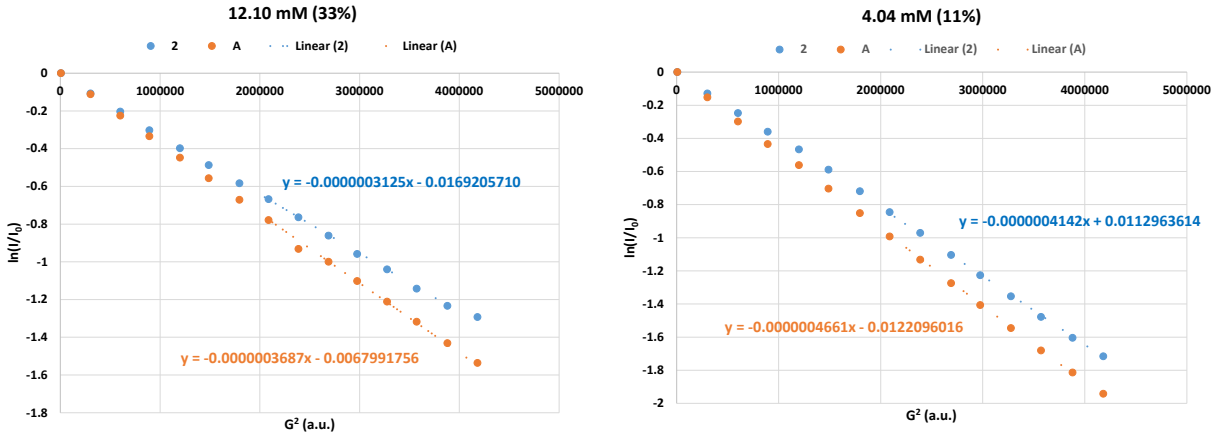

Figure S16. Plot of $\ln(I/I_0)$ vs G^2 for the reference **A** (1,3,5-tri-*tert*-butylbenzene) and **2** in the same graph for a three-fold dilution (left) and nine-fold dilution (right).

r_{PGSE} (**2**, 12 mM) = 4.77 × (36.87/31.25) Å = 5.62 Å (at 0.012 mM)

V_{PGSE} (**2**, 12 mM) = $\frac{4}{3}\pi r^3$ = 747 Å^3

r_{PGSE} (**2**, 4 mM) = 4.77 × (46.61/41.42) Å = 5.37 Å (at 0.004 mM)

V_{PGSE} (**2**, 4 mM) = $\frac{4}{3}\pi r^3$ = 648 Å^3

❖ PGSE DATA FITTING

The decrease in molecular volume observed upon dilution is interpreted as resulting from increased dissociation of the dimer $(\mathbf{2})_2$ upon dilution. In turn, the data can be used to estimate the association constant K as follows ($2 \times C_0$ = total concentration in **2**, M = monomer or **2**, D = dimer or $(\mathbf{2})_2$):

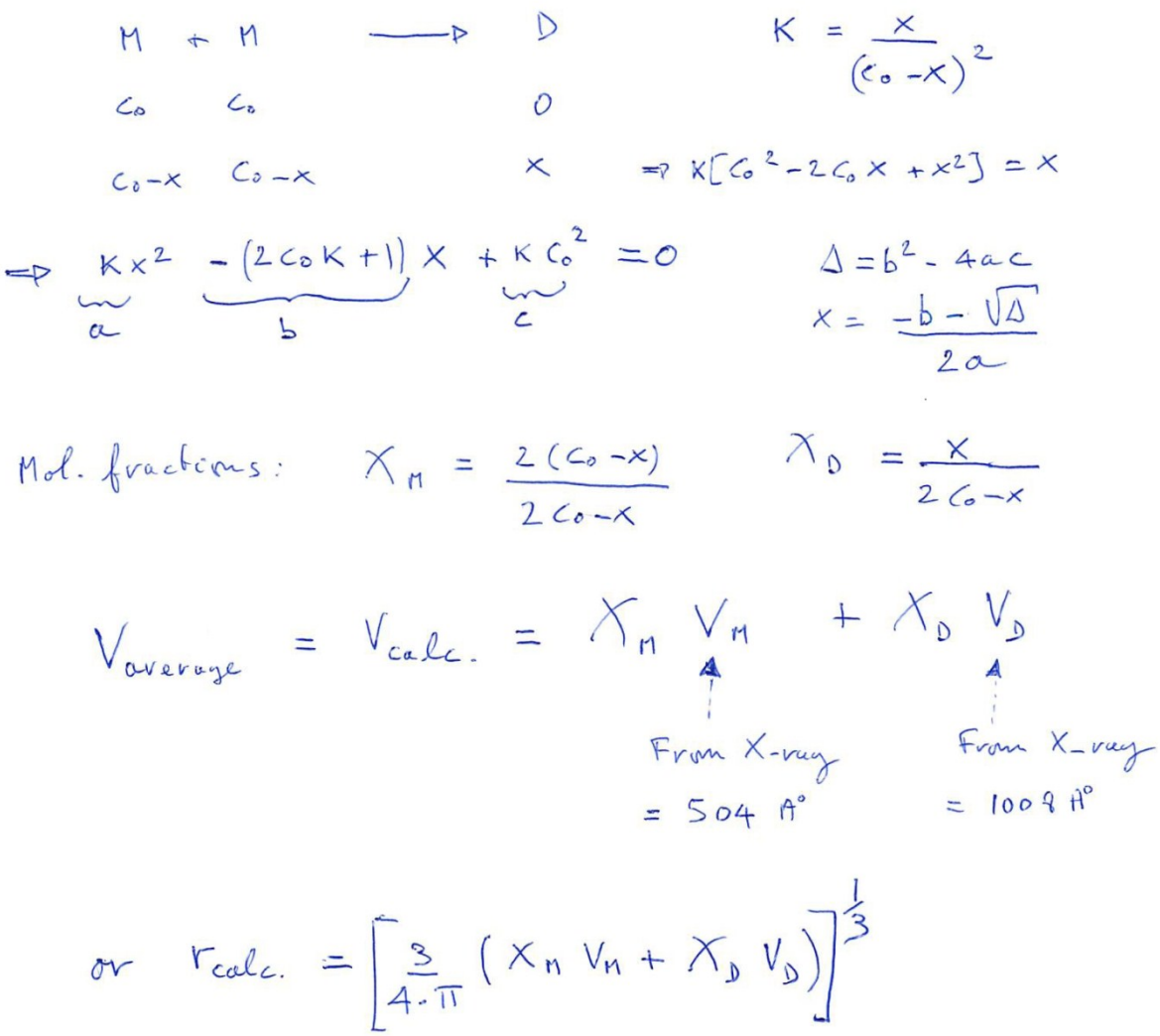

Using this equation, $\mathbf{r_{calc}}$ was fitted against $\mathbf{r}_{PGSE}$ by variation of K. The fitting was performed manually affording K = 1020(±100) M^{-1}. The fitted data is presented in Table S1 along with corresponding volumes. The graph shows the variation of the observed and fitted hydrodynamic radii as a function of concentration.

Table S1. Observed and calculated volumes and radii for 2

Total Concentration (M)	V_{calc}	r_{calc}	V_{PGSE}	r_{PGSE}
0.036	834.62333	5.84172	864.233	5.91
0.012	757.49588	5.655929	747.1255	5.63
0.04	673.4802	5.43858	648.3227	5.37

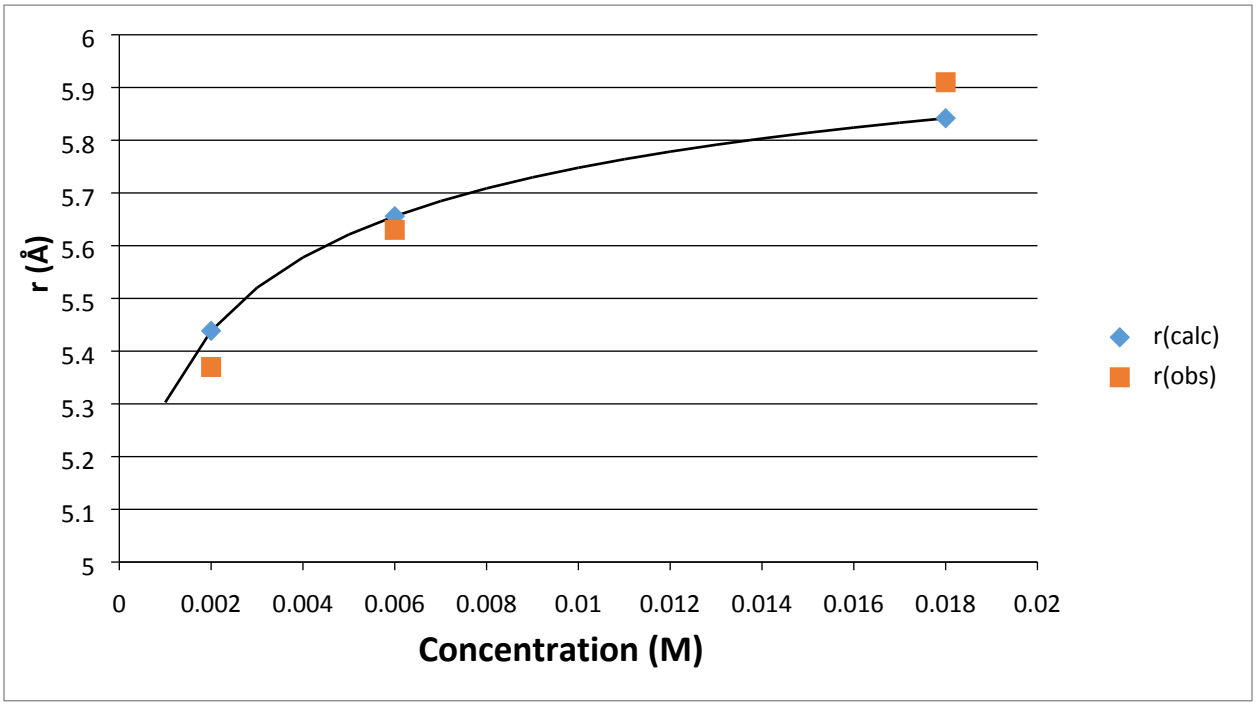

Figure S17. Observed and fitted hydrodynamic radii of **2** in CD_2Cl_2 as a function of concentration.

❖ **Conductivity Measurements.**

The conductivity of solutions of **2** in CH_2Cl_2 at concentrations of 1.0 mM, 0.5mM and 0.1 mM were recorded. The conductivity of these solutions did not differ from that of pure CH_2Cl_2 (Conductivity = 0.00 µS/cm) within experimental error. To assess the reliability of the measurement, CH_2Cl_2 solutions of tetrabutylammonium hexafluorophosphate (1:1 electrolyte) were prepared and their conductivity was measured under same conditions. At the same concentrations, the conductivity of $TBAPF_6$ solutions was significantly higher than that observed for **2** indicating the non-electrolytic nature of **2**. Extrapolation to infinite dilutions using the data obtained for [$TBAPF_6$] = 0.1, 0.5, 1 mM affords Λ_0 = 115 S cm^2 mol^{-1} which is in good agreement with the literature value (109 S cm^2 mol^{-1}).[5]

Table S2. Conductivity of solutions of complex 2 and the reference electrolyte $TBAPF_6$

Concentration of 2 (mM)	Conductivity (µS/cm)
1	0.31
0.5	0.14
0.1	0.00

Concentration of $TBAPF_6$ (mM)	Conductivity (µS/cm)	Molar Conductivity (S cm^2 mol^{-1})
100	1466.00	14.66
10	154.00	15.4
1	33.60	33.6
0.5	22.00	44
0.1	7.67	76.7

❖ LOW RESOLUTION MS-ESI$^-$

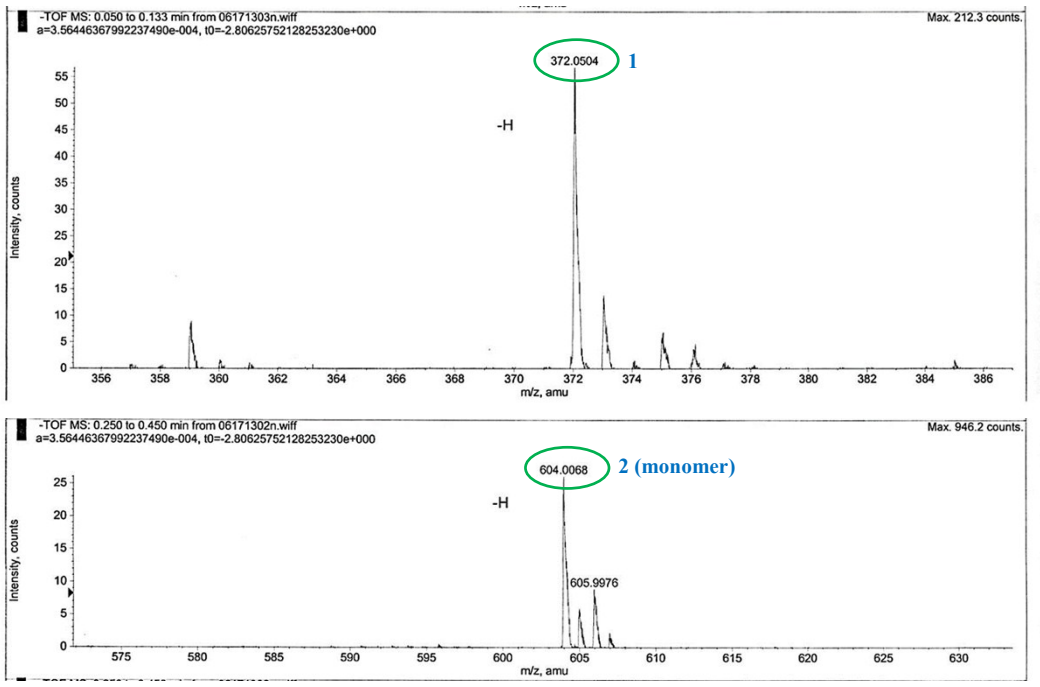

Figure S 18. ESI-MS$^-$ spectra of the ligand **1** (top) and **2** (bottom).

❖ **CATALYSIS OF PROPARGYLIC AMIDES MONITORED BY GC:**

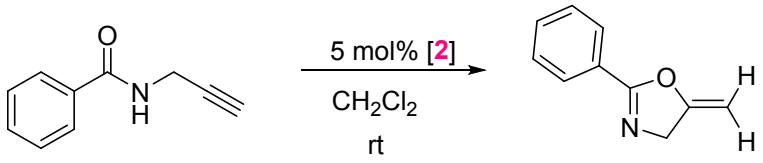

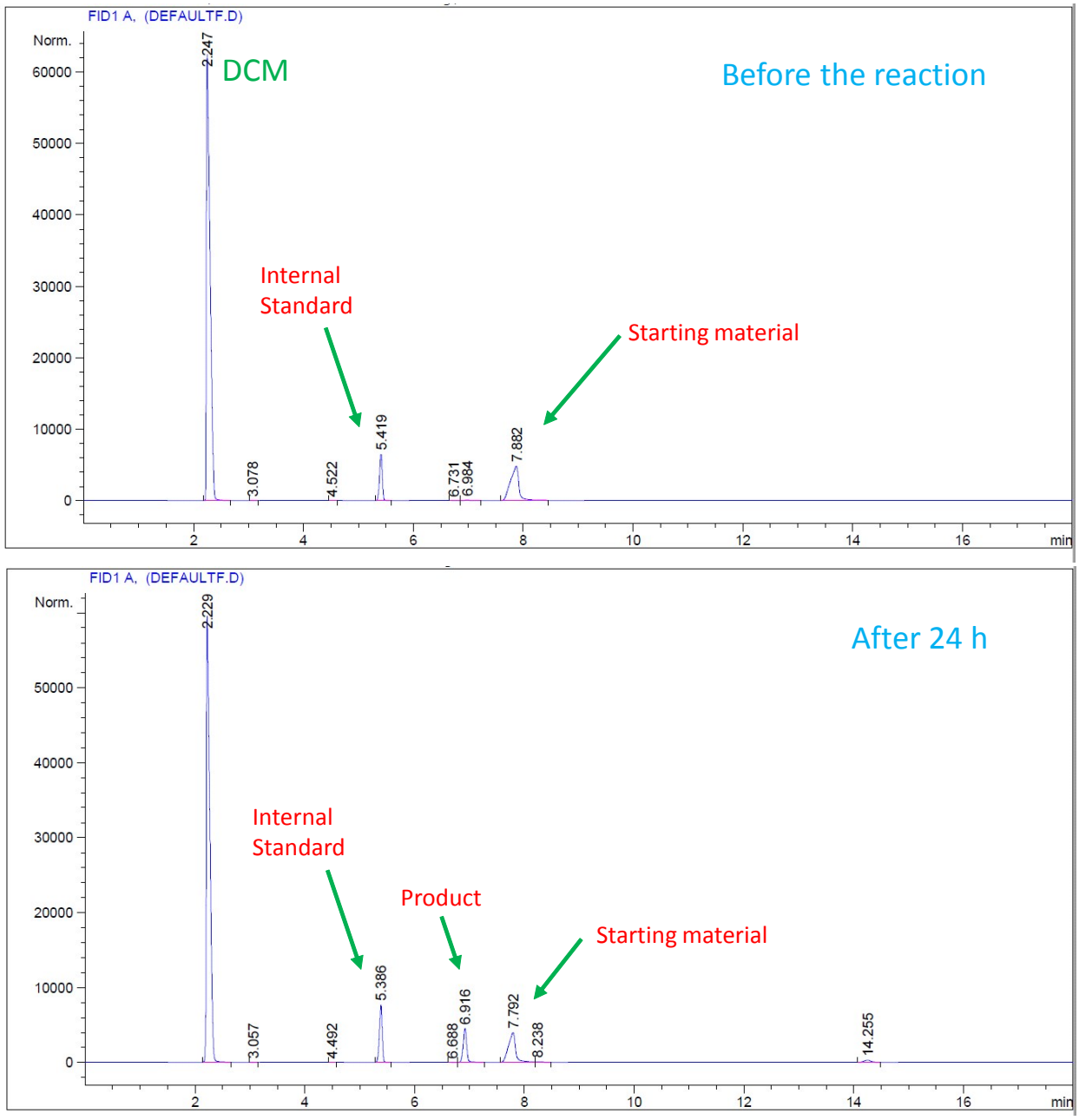

Figure S19. GC trace obtained for the cyclization of N-(prop-2-yn-1-yl)-benzamide catalyzed by **2** in CH_2Cl_2.

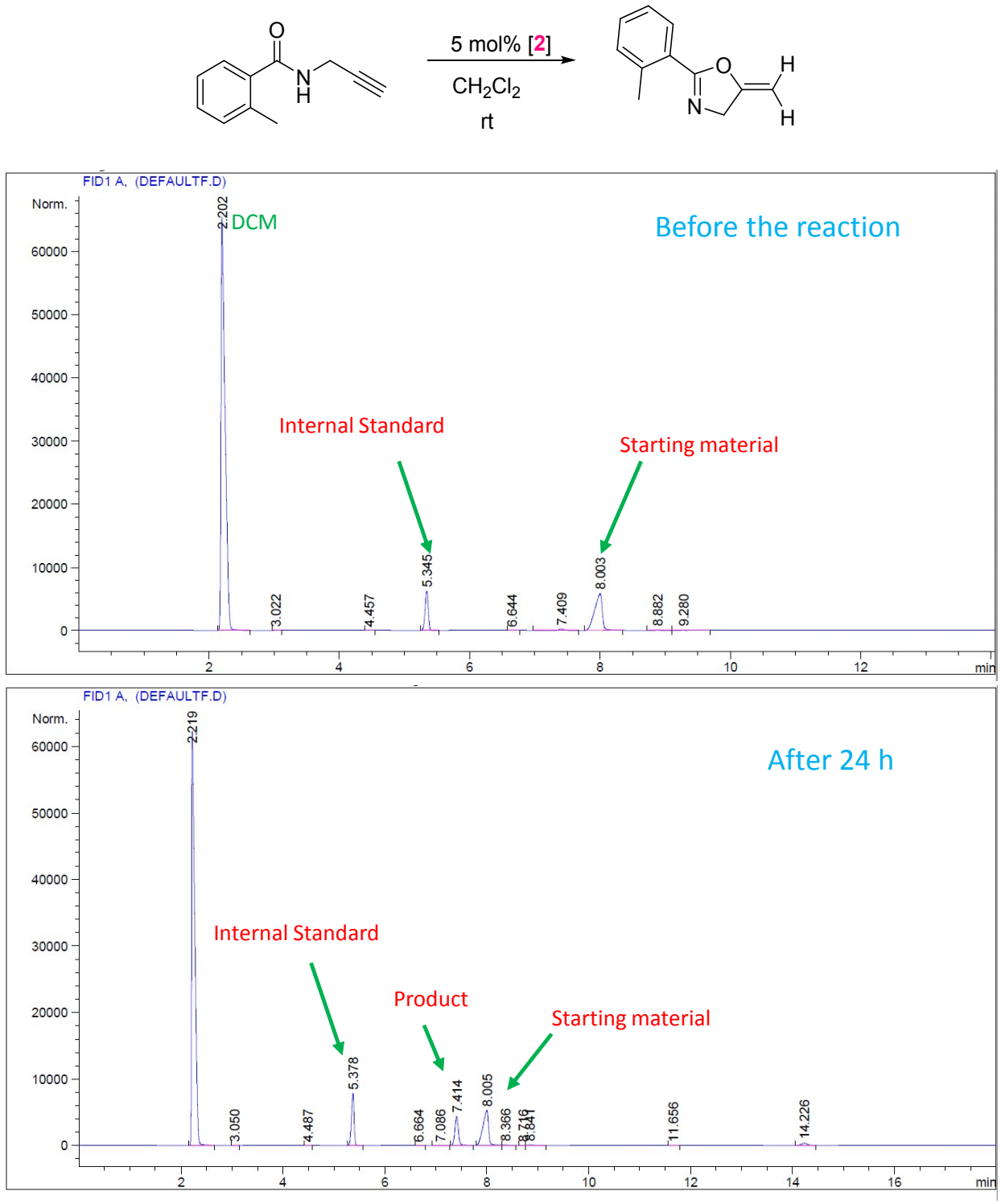

Figure S20. GC trace obtained for the cyclization of N-(prop-2-yn-1-yl)-2-methylbenzamide catalyzed by **2** in CH_2Cl_2.

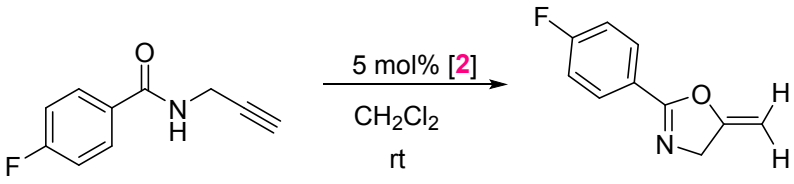

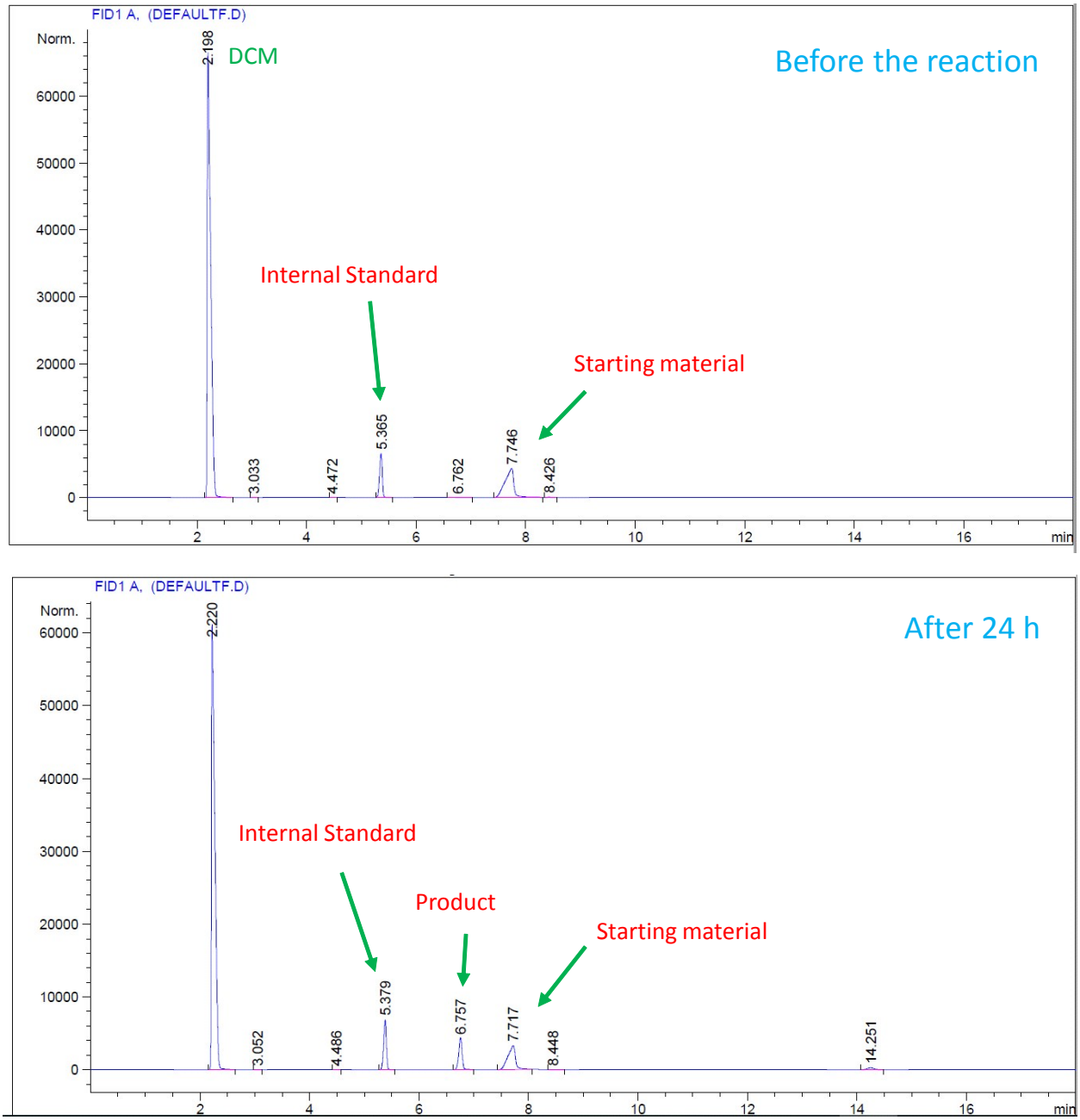

Figure S21. GC trace obtained for the cyclization of N-(prop-2-yn-1-yl)-4-fluorobenzamide catalyzed by **2** in CH_2Cl_2.

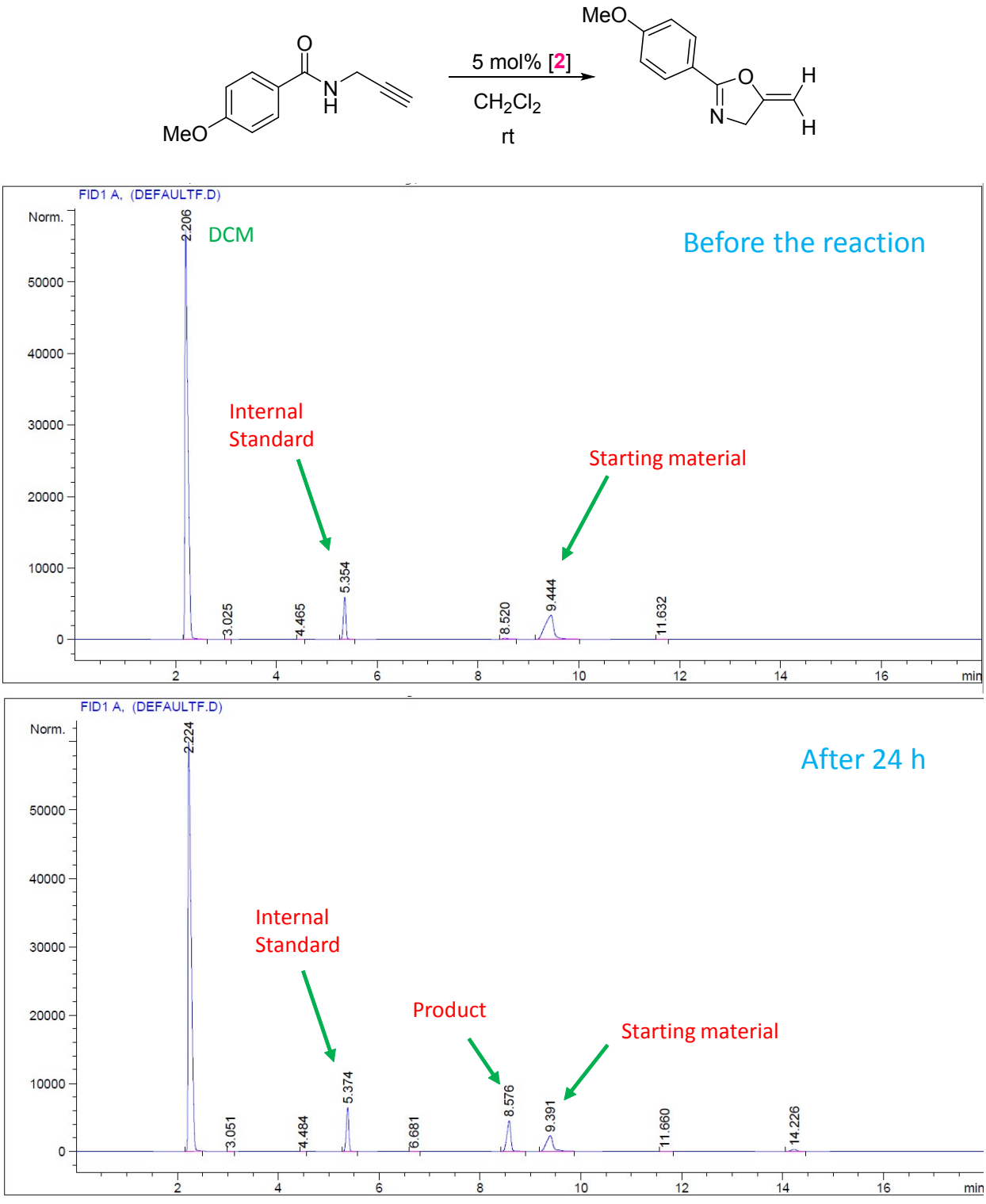

Figure S22. GC trace obtained for the cyclization of N-(prop-2-yn-1-yl)-4-methoxybenzamide catalyzed by **2** in CH_2Cl_2.

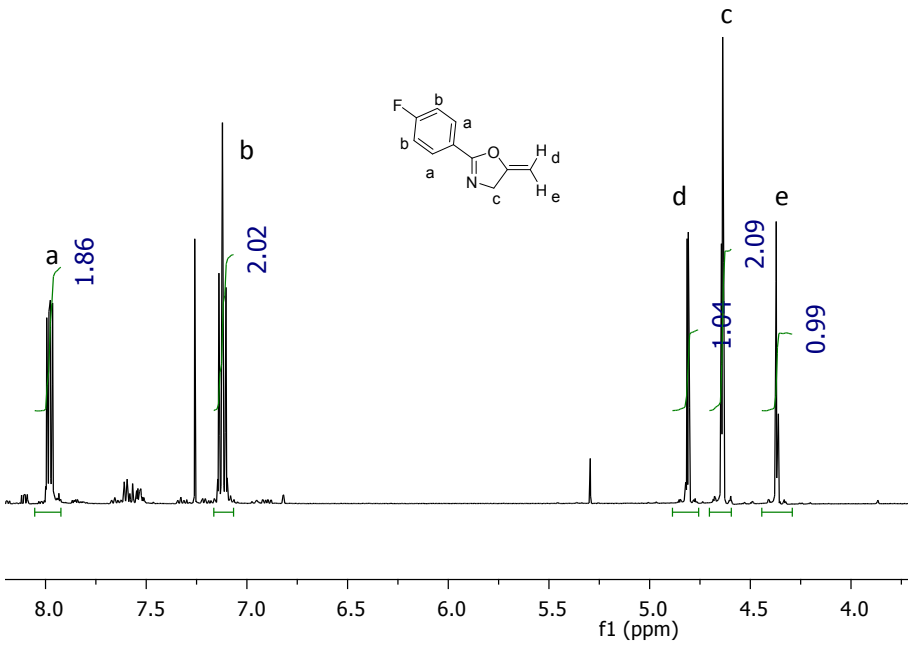

Figure S23. [1]H NMR spectrum of N-(prop-2-yn-1-yl)-4-fluorobenzamide after the completion of the catalysis.

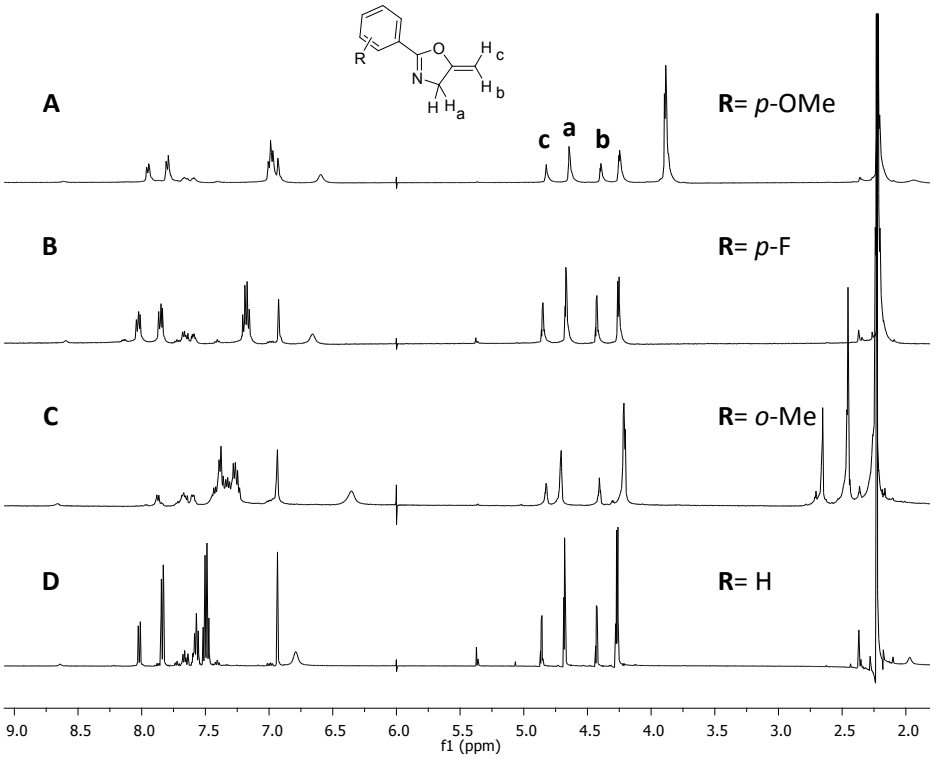

Figure S24. [1]H NMR spectra obtained after 24h for the cyclization of propargylamides catalyzed by **2** in CH_2Cl_2.

References:

1. E. E. Korshin, G. Leitus, L. J. W. Shimon, L. Konstantinovski, D. Milstein, *Inorg. Chem.* 2008, **47**, 7177-7189.
2. C. Pietraszuk, S. Rogalski, B. Powała, M. Miętkiewski, M. Kubicki, G. Spólnik, W. Danikiewicz, K. Woźniak, A. Pazio, A. Szadkowska, A. Kozłowska, K. Grela, *Chem. Eur. J.* 2012, **18**, 6465-6469.
3. U. Huchel, P. Tiwari, R. R. Schmidt, *J. Carbohydr. Chem.* 2010, **29**, 61-75.
4. J. P. Weyrauch, A. S. K. Hashmi, A. Schuster, T. Hengst, S. Schetter, A. Littmann, M. Rudolph, M. Hamzic, J. Visus, F. Rominger, W. Frey, J. W. Bats, *Chem. Eur. J.* 2010, **16**, 956-963.
5. R. J. LeSuer, C. Buttolph, W. E. Geiger, *Anal. Chem.* 2004, **76**, 6395-6401.